Leptogenesis and dark matter detection in a TeV scale neutrino mass model with inverted mass hierarchy

KANAZAWA-13-01
April, 2013

Leptogenesis and dark matter detection in a TeV scale neutrino mass model with inverted mass hierarchy

Shoichi Kashiwase[1] and Daijiro Suematsu[2]

Institute for Theoretical Physics, Kanazawa University,
Kanazawa 920-1192, Japan

Abstract

Realization of the inverted hierarchy is studied in the radiative neutrino mass model with an additional doublet, in which neutrino masses and dark matter could be induced from a common particle. We show that the sufficient baryon number asymmetry is generated through resonant leptogenesis even for the case with rather mild degeneracy among TeV scale right-handed neutrinos. We also discuss the relation between this neutrino mass generation mechanism and low energy experiments for the DM direct search, the neutrinoless double β decay and so on.

[1]e-mail: shoichi@hep.s. kanazawa-u.ac.jp
[2]e-mail: suematsu@hep. s.kanazawa-u.ac.jp

1 Introduction

The existence of small neutrino masses [1] and dark matter (DM) [2] gives us important clues to consider physics beyond the standard model (SM). It is interesting that various recent works clarify a certain type of models can relate them closely. Such typical examples are neutrino models in which neutrino masses are radiatively generated at TeV regions. There, this characteristic feature is caused by a symmetry which forbids the generation of the Dirac neutrino masses at tree-level and guarantees the stability of new neutral particles, simultaneously. A stable particle among them might be DM. Since both the relic abundance of DM and the neutrino oscillation data severely constrain the relevant model parameters in general, the viability of such scenarios is expected to be checked through near future experiments at TeV or lower energy regions.

A concrete model can be constructed on the basis of the radiative seesaw mechanism proposed in [3]. It is a very simple extension of the SM by an additional doublet scalar and three right-handed neutrinos only.[3] A Z_2 symmetry is introduced in the model such that the SM contents have even parity and the new particles have odd parity. Then, it can forbid the generation of neutrino masses at tree-level and also guarantees the stability of the lightest Z_2 odd particle which could be DM. In this model, we can consider various possible scenarios depending on the spectrum of new particles which determines a DM candidate [4, 5, 6].[4]

If the lightest right-handed neutrino is identified with the DM, its neutrino Yukawa couplings are generally required to take large values. In such a case, both the lepton flavor violating processes and the relic abundance of DM can easily contradict each other [4]. In order to evade this problem, we need to assume special flavor structure or introduce some new interaction at TeV regions [5]. In the thermal leptogenesis due to the decay of the right-handed neutrinos [8, 9], the washout of the generated lepton asymmetry is too effective to yield the required baryon number asymmetry in this case . We need to consider non-thermal leptogenesis [10] or resonant leptogenesis [11].

On the other hand, if the lightest neutral component of the inert doublet scalar is identified with DM, this problem can be escaped.[5] Since the scalar quartic couplings

[3]We call this new doublet the inert doublet hereafter, although it has Yukawa couplings with neutrinos.

[4]Supersymmetric extension has also been considered in [7].

[5]The inert doublet DM has been studied in a lot of papers [12].

effectively cause their (co)annihilation, the neutrino Yukawa couplings could be irrelevant to the DM relic abundance [13]. Thus, the lepton flavor violating processes do not impose substantial constraints on the model in this case. Thus, if we consider the leptogenesis there, the washout of the generated lepton number asymmetry can be suppressed by making the neutrino Yukawa couplings small enough. The model has been shown to explain the DM abundance and the baryon number asymmetry in a consistent way with the neutrino oscillation data assuming the normal hierarchy in [14]. Although the resonant effect is indispensable to enhance the CP asymmetry sufficiently, the degeneracy required for the right-handed neutrino masses is found to be rather mild there.

In this paper we extend the study in [14] to the inverted neutrino mass hierarchy. We examine whether all the neutrino oscillation data and the baryon number asymmetry can be consistently explained also in such a framework. We also discuss how the generation mechanism of the neutrino masses in this model could be related to near future experiments for a direct DM search and also the neutrinoless double β decay.

The following parts are organized as follows. In section 2 we briefly introduce the model and discuss the realization of the inverted neutrino mass hierarchy. We also address the necessary conditions to consider the thermal leptogenesis in this model. In section 3 we give the result of the numerical analysis of the baryon number asymmetry. Taking account of this result, the relation between this neutrino mass generation mechanism and the phenomena at the low energy region such as the DM scattering with nucleus and the neutrinoless double β decay is discussed. The conclusion of the paper is given in section 4.

2 Inverted mass hierarchy in a radiative neutrino mass model

We consider a simple extension of the standard model (SM) which is proposed for the neutrino mass generation at one-loop level [3]. In this model, only three right-handed neutrinos N_i and an inert doublet scalar η are added to the SM as new ingredients. Although both N_i and η are supposed to have odd parity of an assumed Z_2 symmetry, all SM contents are assigned its even parity. Z_2 invariant Yukawa couplings and scalar

potential related to these new fields are summarized as

$$\begin{aligned} -\mathcal{L}_Y &= h_{\alpha i}\bar{N}_i\eta^\dagger\ell_\alpha + h^*_{\alpha i}\bar{\ell}_\alpha\eta N_i + \frac{M_i}{2}\bar{N}_i N_i^c + \frac{M_i}{2}\bar{N}_i^c N_i, \\ V &= m_\phi^2\phi^\dagger\phi + m_\eta^2\eta^\dagger\eta + \lambda_1(\phi^\dagger\phi)^2 + \lambda_2(\eta^\dagger\eta)^2 + \lambda_3(\phi^\dagger\phi)(\eta^\dagger\eta) \\ &+ \lambda_4(\eta^\dagger\phi)(\phi^\dagger\eta) + \left[\frac{\lambda_5}{2}(\phi^\dagger\eta)^2 + \text{h.c.}\right], \end{aligned} \tag{1}$$

where ℓ_α is a left-handed lepton doublet and ϕ is an ordinary Higgs doublet with $|\langle\phi\rangle| = 174$ GeV. Yukawa couplings are written by using the basis, under which both matrices of the right-handed neutrino masses and the Yukawa couplings of charged leptons are real and diagonal. Since the new doublet scalar η is assumed to have no vacuum expectation value, the Z_2 symmetry is remained as the exact symmetry. It forbids the neutrinos to have Yukawa interactions with the ordinary Higgs scalar ϕ. As a result, neutrino masses are not generated at tree-level as found from eq. (1). The lightest field with odd parity of this Z_2 symmetry is stable and then its thermal relics behave as DM in the Universe. If the lightest neutral component of η is identified with DM, it is found that its (co)annihilation caused by the scalar quartic couplings λ_3 and λ_4 can determine its relic abundance [13, 14]. In this case, since the DM abundance gives no constraint on the neutrino Yukawa couplings, the model can be easily consistent with other phenomenological constraints such as the ones caused by the lepton flavor violating processes. We follow this scenario in this paper, and η_R is assumed to be DM which requires $\lambda_5 < 0$ and $\lambda_4 < 0$ [14].

Neutrino masses are generated through one-loop diagrams with the contribution of the Z_2 odd particles. They can be expressed as

$$\mathcal{M}^\nu_{\alpha\beta} = \sum_{k=1}^{3} h_{\alpha k}h_{\beta k}\Lambda_k. \tag{2}$$

Scales for the neutrino masses are considered to be fixed by Λ_k, which is defined as

$$\Lambda_k = \frac{\lambda_5\langle\phi\rangle^2}{8\pi^2 M_k}\frac{M_k^2}{M_\eta^2 - M_k^2}\left(1 + \frac{M_k^2}{M_\eta^2 - M_k^2}\ln\frac{M_k^2}{M_\eta^2}\right), \tag{3}$$

where $M_\eta^2 = m_\eta^2 + (\lambda_3 + \lambda_4)\langle\phi\rangle^2$.[6] This shows that neutrino Yukawa couplings could have rather large values even for the light right-handed neutrinos with the mass of $O(1)$ TeV as long as $|\lambda_5|$ takes a small value.

[6]We note that the λ_5 contribution in this formula for M_η^2 is neglected, since λ_5 is assumed to be sufficiently small.

Now we consider the realization of the inverted hierarchy in this mass formula. For this purpose, we may start the study from the neutrino mass matrix which brings the tri-bimaximal mixing.[7] Since the recent experiments suggest nonzero θ_{13} [15], it can be just an approximation for the realistic mixing. However, we use it as a convenient starting point of the study and introduce suitable modifications to it so as to realize a favorable value for θ_{13}. Taking this strategy, we assume that the neutrino Yukawa couplings have the following flavor structure [5]:

$$h_{e1} = -2h_{\mu 1} = 2h_{\tau 1} = 2h_1; \quad h_{e2} = h_{\mu 2} = -h_{\tau 2} = h_2; \quad h_{e3} = 0,\ h_{\mu 3} = h_{\tau 3} = h_3. \tag{4}$$

This flavor structure for the neutrino Yukawa couplings induces a following simple form for the neutrino mass matrix:

$$\mathcal{M}^\nu = \begin{pmatrix} 4 & -2 & 2 \\ -2 & 1 & -1 \\ 2 & -1 & 1 \end{pmatrix} h_1^2\Lambda_1 + \begin{pmatrix} 1 & 1 & -1 \\ 1 & 1 & -1 \\ -1 & -1 & 1 \end{pmatrix} h_2^2\Lambda_2 + \begin{pmatrix} 0 & 0 & 0 \\ 0 & 1 & 1 \\ 0 & 1 & 1 \end{pmatrix} h_3^2\Lambda_3. \tag{5}$$

As easily found, this matrix can be diagonalized as $U_{\rm PMNS}^T \mathcal{M}^\nu U_{\rm PMNS} = {\rm diag}(m_1,\ m_2,\ m_3)$ by using the tri-bimaximal PMNS matrix

$$U_{\rm PMNS} = \begin{pmatrix} \frac{2}{\sqrt{6}} & \frac{1}{\sqrt{3}} & 0 \\ \frac{-1}{\sqrt{6}} & \frac{1}{\sqrt{3}} & \frac{1}{\sqrt{2}} \\ \frac{1}{\sqrt{6}} & \frac{-1}{\sqrt{3}} & \frac{1}{\sqrt{2}} \end{pmatrix} \begin{pmatrix} e^{i\alpha_1} & 0 & 0 \\ 0 & e^{i\alpha_2} & 0 \\ 0 & 0 & 1 \end{pmatrix}. \tag{6}$$

The mass eigenvalues are expressed as

$$m_1 = 6|h_1^2\Lambda_1|, \qquad m_2 = 3|h_2^2\Lambda_2|, \qquad m_3 = 2|h_3^2\Lambda_3|. \tag{7}$$

Majorana phases $\alpha_{1,2}$ are determined by the phases $\varphi_i = \arg(h_i)$ as

$$\alpha_1 = \varphi_1 - \varphi_3, \qquad \alpha_2 = \varphi_2 - \varphi_3. \tag{8}$$

[7] In this paper we do not assume any flavor symmetry to realize this structure. Thus, the quantum corrections could change it. However, since the assumed neutrino Yukawa couplings are very small, the zero texture of these neutrino Yukawa couplings are expected to be kept in good accuracy after taking account of the quantum effects through the renormalization group equations. Thus, if the values of nonzero neutrino Yukawa couplings at high energy scale are set suitably, the results obtained in this study could be reproduced. The detailed analysis is beyond the scope of the present study and it will be given elsewhere.

where $\langle\phi\rangle$ is assumed to be real and positive.

Here we impose the neutrino oscillation data on the model. They are well-known to be explained by the two types of mass hierarchy which are called the normal hierarchy and the inverted hierarchy. In the present model, these possibilities are realized in the following way. In the former case, the mass eigenvalues should satisfy

$$m_3^2 - m_1^2 = \Delta m^2_{\rm atm}, \qquad m_2^2 - m_1^2 = \Delta m^2_{\rm sol}, \tag{9}$$

where $\Delta m^2_{\rm atm}$ and $\Delta m^2_{\rm sol}$ stand for squared mass differences required by the neutrino oscillation analysis for atmospheric and solar neutrinos, respectively [1, 16, 17]. This case has been investigated from various phenomenological points of view [4, 5, 6, 14]. Through this study, it is shown that all the neutrino masses, mixing and the DM abundance are successfully explained. However, the generation of the baryon number asymmetry due to thermal leptogenesis is difficult unless the resonance effect is taken into account. On the other hand, in the latter case, the mass eigenvalues should satisfy

$$\Delta m^2_{13} \equiv m_1^2 - m_3^2 = \Delta m^2_{\rm atm}, \qquad \Delta m^2_{21} \equiv m_2^2 - m_1^2 = \Delta m^2_{\rm sol}. \tag{10}$$

Although this case is expected to have interesting features which are different from those of the normal hierarchy, it seems not to have been studied well in this model yet. We focus our attention on this case in the remaining part.

Before considering the concrete realization of the inverted hierarchy, we first address necessary conditions which should be satisfied for the thermal leptogenesis brought through the decay of the lightest right-handed neutrino in this framework. The lightest neutral component of η which has the mass in the TeV region is known to satisfy the required DM relic abundance as long as the quartic couplings λ_3 or λ_4 have the sufficient magnitude [13, 14]. In that case, its relic abundance is determined only by these couplings. Since neutrino Yukawa couplings play no role in this determination, the relic DM abundance has no relation with the neutrino mass eigenvalues as found from eqs. (2) and (3) as in the normal hierarchy case. We follow this scenario and assume that $M_\eta < M_{1,2,3}$ is satisfied. In this case, the present direct searches of DM [18, 19] impose the constraint on λ_5 and $\lambda_3 + \lambda_4$.

The bound for $|\lambda_5|$ appears from the inelastic scattering between $\eta^0_{R,I}$ and a nucleus through Z^0 exchange which could contribute to direct search experiments. The differential scattering rate for recoil nucleus energy E_R crucially depends on the DM velocity

distribution and it has a relation such as [20]

$$\frac{dR}{dE_R} \propto \sigma_n^0 \int_{v_{\rm min}}^{v_{\rm esc}} d^3v \ \frac{f(v)}{v}, \tag{11}$$

where $f(v)$ is the DM velocity distribution function and σ_n^0 is the DM-nucleon scattering cross section with zero momentum transfer. Since η_R^0 and η_I^0 have mass difference δ, the scattering occurs only for the DM velocity larger than [21]

$$v_{\rm min} = \frac{1}{\sqrt{2m_N E_R}} \left(\frac{E_R m_N}{m_r} + \delta \right), \tag{12}$$

where m_N is the mass of a target nucleus and m_r is the reduced mass of DM and the nucleus. Upper bound of the DM velocity is determined as the escape velocity from the galaxy and it is estimated as $v_{\rm esc} = 544$ km/s. In Fig. 1, we plot the present Xenon100 bound on σ_n^0 as a function of δ. The lines representing this bound are found to have an end point for large values of δ. This is caused since $v_{\rm esc} < v_{\rm min}$ occurs there. In that case, the inelastic scattering is kinematically forbidden due to the existence of the upper bound of DM velocity $v_{\rm esc}$. Since σ_n^0 for this inelastic scattering is estimated as $\sigma_n^0 \simeq \frac{1}{2\pi} G_F^2 m_n^2 \sim 7.4 \times 10^{-39}$ cm^2 and $\delta \equiv m_{\eta_I} - m_{\eta_R} \simeq \frac{|\lambda_5|\langle\phi\rangle^2}{m_{\eta_R}}$, we find that $|\lambda_5|$ is constrained from Fig. 1 as [22]

$$|\lambda_5| \simeq \frac{M_\eta \delta}{\langle\phi\rangle^2} \ \gtrsim \ 6.7 \times 10^{-6} \left(\frac{M_\eta}{1 \text{ TeV}} \right) \left(\frac{\delta}{200 \text{ keV}} \right). \tag{13}$$

This bound affects the neutrino Yukawa couplings through the neutrino oscillation data if we recall the present neutrino mass generation mechanism represented by eqs. (2) and (3).

The elastic scattering due to the Higgs exchange can also be a target of the direct search. The present direct search results impose the constraint on the value of $\lambda_3 + \lambda_4$, since the DM-nucleon scattering cross section for this process is estimated as

$$\sigma_n^0 = \frac{(\lambda_3 + \lambda_4 + \lambda_5)^2}{8\pi} \frac{m_n^2 f_n^2}{m_{\eta_R}^2 m_h^4}. \tag{14}$$

The present bound obtained by Xenon100 gives the constraint such as

$$|\lambda_3 + \lambda_4 + \lambda_5| \lesssim 1.8 \left(\frac{m_{\eta_R}}{1 \text{ TeV}} \right), \tag{15}$$

where we use $m_h = 125$ GeV and $f_n = 1/3$. This bound could be intimately related to the relic density of η_R [14]. It may be useful to note that this condition can be easily

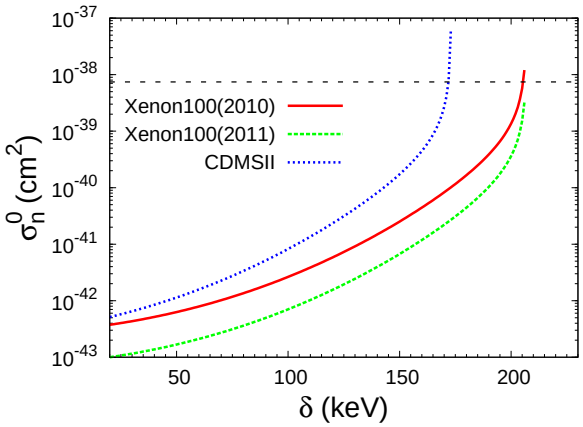

Fig. 1 Direct detection constraint for the mass difference δ between η_R and η_I. The bound of the DM-nucleon cross section obtained in each experiment is drawn. In this plot we use $E_R = 40$ keV, as an example.

satisfied in the case $\lambda_3\lambda_4 < 0$ even for $|\lambda_{3,4}| = O(1)$, which is favored to reduce effectively the η_R relic density to the required value. This point will be discussed in the relation to the DM detection at the Xenon1T experiment in the latter part again.

On the other hand, thermal leptogenesis requires that the decay of the lightest right-handed neutrino N_i should occur in the out-of-thermal equilibrium. This imposes the condition such that $H > \Gamma^D_{N_i}$ has to be satisfied at $T \lesssim M_i$, where H and $\Gamma^D_{N_i}$ are the Hubble parameter and the decay width of N_i, respectively. From this condition, we find that the Yukawa coupling of N_i should be small enough as

$$|h_i| < O(10^{-8}) \left(\frac{M_i}{1\ \text{TeV}}\right)^{1/2}. \tag{16}$$

Here we note that small $|h_i|$ guarantees that N_i is irrelevant to the determination of the neutrino masses and the mixing angles. If we apply this condition to eqs. (7) and (10), we find that the lightest right-handed neutrino should be N_3 in the present case. This means that both $|h_3| < O(10^{-8})$ and $M_3 < M_{1,2}$ should be satisfied. Since the resonant leptogenesis is considered to be crucial for the generation of the sufficient baryon number asymmetry as in the normal hierarchy case, we can suppose two scenarios defined by the following spectrum of the right-handed neutrinos here:

$$\text{(i)}\ M_3 \lesssim M_1 < M_2, \qquad \text{(ii)}\ M_3 \lesssim M_2 < M_1, \tag{17}$$

where the first inequality represents that these masses are almost degenerate each other

in each case.[8]

We present a brief comment on the degenerate masses of the right-handed neutrinos.[9] They could be obtained without disturbing the flavor structure of $\mathcal{L}_Y$ in eq. (1), if their mass terms take a form such as

$$\mathcal{L}_{\mathcal{M}} = \frac{M}{2}\left(\bar{N}_3 N_3^c + \bar{N}_i N_i^c\right) + \frac{M_j}{2}\bar{N}_j N_j^c + \frac{\Delta_i}{2} M \bar{N}_3 N_i^c + \text{h.c.}, \tag{18}$$

where $\Delta_i \ll 1$ is assumed. It is useful to note that this structure for the right-handed neutrino masses could be realized by supposing the model with the fifth dimension. If we assume that the right-handed neutrinos localize around the different fifth dimensional points and other fields are distributed throughout the fifth dimensional direction, the neutrino sector in the effective 4-dimensional model obtained after integrating out the fifth coordinate can have the feature described by $\mathcal{L}_Y$ and $\mathcal{L}_M$.[10] The small mass mixing between N_3 and N_i is explained by the small overlapping of their wave function in the direction of the fifth dimension. In the case described by eq. (18), the mass eigenstates in the mixed sector can be identified with N_3 and N_i to a good accuracy and their mass eigenvalues are $M_3 = M(1 - \frac{\Delta_i}{2})$ and $M_i = M(1 + \frac{\Delta_i}{2})$. Using the mass eigenvalues, Δ_i is expressed as $\Delta_i = \frac{M_i}{M_3} - 1$. If we take $i = 1$ and $j = 2$, for example, the case (i) is realized.

Now we fix the framework to realize the inverted hierarchy which can explain the neutrino oscillation data. Recent experiments show that the mixing angle θ_{13} is not zero but has a rather large value [15]. In order to make the explanation of these data possible in the model, the flavor structure (4) has to be changed. Although there are a lot of way to introduce the modification for it, we take a simple scheme such that eq. (4) is deformed by new real free parameters $p_{1,2}$ and $q_{1,2}$ as

$$h_{e1}/p_1 = -2h_{\mu 1}/q_1 = 2h_{\tau 1} = 2h_1; \quad h_{e2}/p_2 = h_{\mu 2}/q_2 = -h_{\tau 2} = h_2. \tag{19}$$

Since the smallness of $|h_3|$ guarantees that N_3 is irrelevant to the neutrino masses and

[8] It is possible to consider the situation such that three right-handed neutrinos are all degenerate. However, we do not consider this case here since the result can be estimated by using the results of the two cases.

[9] Other scenarios for tiny mass splittings of the right-handed neutrino can be found in [23].

[10] Although the high degeneracy of the right-handed neutrino masses might be explained in this way, the required values for Yukawa couplings in $\mathcal{L}_Y$ should be just assumed in this framework.

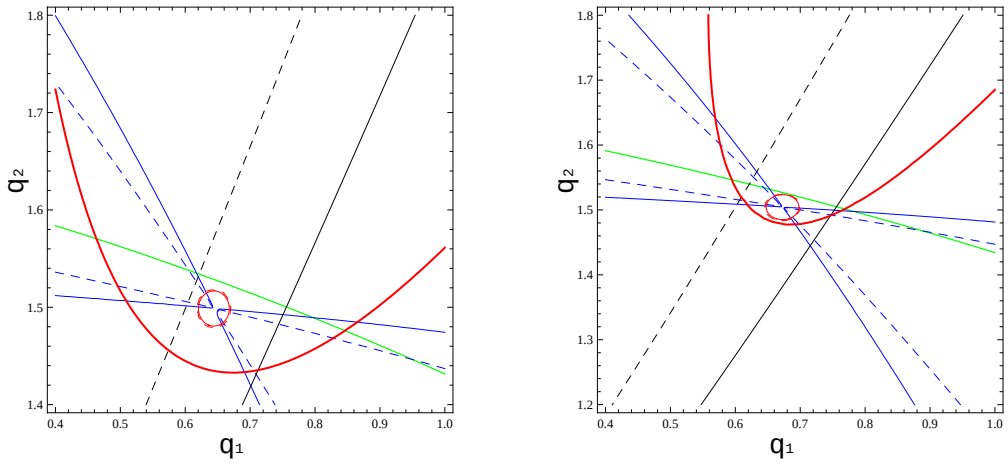

Fig. 2 Allowed region in the (q_1, q_2) plane by the neutrino oscillation data. Left and right panels correspond to the cases (i) and (ii) shown in Table 1, respectively. Each contour in both panels represents neutrino oscillation parameters Δm^2_{13} (thick red lines), Δm^2_{21} (thin red lines), $\sin^2 2\theta_{23}$ (green lines), $\sin^2 2\theta_{12}$ (blue lines), and $\sin^2 2\theta_{13}$ (black lines) for the 2σ values given in [17]. For each of the parameters, the upper and lower bounds are expressed by the dashed and solid lines, respectively.

mixing, the neutrino mass matrix can be written as

$$\mathcal{M}^\nu \simeq \begin{pmatrix} 4p_1^2 & -2p_1q_1 & 2p_1 \\ -2p_1q_1 & q_1^2 & -q_1 \\ 2p_1 & -q_1 & 1 \end{pmatrix} h_1^2\Lambda_1 + \begin{pmatrix} p_2^2 & p_2q_2 & -p_2 \\ p_2q_2 & q_2^2 & -q_2 \\ -p_2 & -q_2 & 1 \end{pmatrix} h_2^2\Lambda_2. \tag{20}$$

We numerically diagonalize this matrix to find the mass eigenvalues and the mixing angles. The model parameters are determined by comparing these results with the neutrino oscillation data. In Fig. 2, we plot contours in the $(q_1,\ q_2)$ plane for 2σ values of neutrino oscillation parameters given in [17]. In each panel of this figure, a part of parameters is commonly fixed as $M_\eta = 1$ TeV, $M_3 = 2$ TeV and $|\lambda_5| = 10^{-4}$. The values used for other parameters $M_{1,2}$, $|h_{1,2}|$ and $p_{1,2}$ are shown in Table 1. In this figure, we find that the allowed regions are displayed as four sectors on the small circle drawn by the thin red lines, which are sandwiched by the blue dashed and solid lines. Values of (q_1, q_2) shown in Table 1 are contained in these regions.[11] The predicted value of $\sin^2 2\theta_{13}$ at this point is also given in this table. This figure shows that the mass matrix derived from the flavor

[11] In this analysis, we find the solutions by varying (q_1, q_2) only, for simplicity. If we vary other parameters to find solutions simultaneously, the tuning of (q_1, q_2) required here is expected to be much mild.

	M_1	M_2	$10^4\|h_1\|$	$10^4\|h_2\|$	(p_1, p_2)	(q_1, q_2)	$\sin^2 2\theta_{13}$	m_{ee}(eV)
(i)	2	8	5.8	9.0	(1.17,0.84)	(0.630,1.515)	0.11	0.0195-0.0486
(ii)	8	2	6.7	7.5	(1.17,0.86)	(0.656,1.521)	0.10	0.0156-0.0473

Table 1 Typical parameters used in this analysis. Other parameters are fixed as $|h_3| = 3 \times 10^{-8}$, $|\lambda_5| = 10^{-4}$, $M_3 = 2$ TeV, and $M_\eta = 1$ TeV.

structure (19) can explain all the neutrino oscillation data, the DM relic abundance and its phenomenology consistently as long as the relevant parameters are fixed suitably.

As shown in these analysis, small neutrino Yukawa couplings $|h_{1,2}|$ of $O(10^{-3})$ can explain the neutrino oscillation data even for the TeV scale values of $M_{1,2}$ and M_η as long as we assume the values of $O(10^{-4})$ for $|\lambda_5|$. Although both the lepton flavor violating processes such as $\mu \to e\gamma$ and the anomalous magnetic momentum of a muon are induced through one-loop diagrams with Z_2 odd particles in the internal lines [24], these contributions could be largely suppressed due to these small neutrino Yukawa couplings. In fact, for the parameters used here, we find that these quantities are negligibly small as follows,

$$\begin{aligned}
\mathrm{Br}(\mu \to e\gamma) &= \frac{3\alpha}{64\pi (G_F M_\eta^2)^2} \left[-2p_1 h_1^2 F_2\left(\frac{M_1}{M_\eta}\right) + p_2 h_2^2 F_2\left(\frac{M_2}{M_\eta}\right)\right]^2 = O(10^{-25\sim-24}), \\
\mathrm{Br}(\tau \to \mu\gamma) &= \frac{3\alpha}{64\pi (G_F M_\eta^2)^2} \left[q_1 h_1^2 F_2\left(\frac{M_1}{M_\eta}\right) + q_2 h_2^2 F_2\left(\frac{M_2}{M_\eta}\right)\right]^2 = O(10^{-24\sim-23}), \\
\delta a_\mu &= \frac{1}{(4\pi)^2}\frac{m_\mu^2}{M_\eta^2} \left[h_1^2 F_2\left(\frac{M_1}{M_\eta}\right) + h_2^2 F_2\left(\frac{M_2}{M_\eta}\right)\right] = O(10^{-18}),
\end{aligned} \tag{21}$$

where $F_2(x) = (1 - 6x^2 + 3x^4 + 2x^6 - 6x^4 \ln x^2)/6(1-x^2)^4$. The present bounds for these lepton flavor violating processes [25] do not impose any constraints on the model. Since the contribution of the new particles to the muon $g-2$ is insufficient to account for the experimental value which deviates from the SM prediction [26], some additional extension of the model is required for that explanation. If we make $|\lambda_5|$ smaller, these values become larger due to the larger neutrino Yukawa couplings. However, as long as the value of $|\lambda_5|$ takes a value in the region given in eq.(13) which is imposed by the DM direct search, these processes can never be targets of future experiments to examine the model unfortunately.

3 Baryon number asymmetry and low energy phenomena

3.1 Resonant leptogenesis

We consider the thermal leptogenesis due to the out-of-equilibrium decay of the right-handed neutrino N_3.[12] In the previous part, we have considered two possible patterns for the masses of the right-handed neutrinos, which are shown in eq. (17). Through this analysis, it has been shown that the model can explain all the neutrino oscillation data in the suitable parameter regions. These typical examples are shown in Fig. 2 and Table 1. Although the mass of N_3 seems to be too small to realize the sufficient CP asymmetry associated with this decay process for the generation of the required baryon number asymmetry, it could be enhanced by the resonance effect as known in the ordinary resonant leptogenesis [27]. The dominant contribution to the CP asymmetry is expected to be caused by the interference between the tree diagram and the one-loop self-energy diagram as usual. The CP asymmetry ε in the N_3 decay is expressed as [27]

$$\varepsilon = \sum_{i=1,2} \frac{\mathrm{Im}(h^\dagger h)^2_{i3}}{(h^\dagger h)_{33}(h^\dagger h)_{ii}} \frac{(M_3^2 - M_i^2)M_3\Gamma_{N_i}}{(M_3^2 - M_i^2)^2 + M_3^2\Gamma_{N_i}^2}, \tag{22}$$

where $\Gamma_{N_i} = \sum_\alpha \frac{|h_{\alpha i}|^2}{8\pi} M_i (1 - \frac{M_\eta^2}{M_i^2})^2$.

The dominant part of ε in each case shown in Table 1 is obtained by substituting $i = 1$ for (i) and $i = 2$ for (ii). Thus, if we use the flavor structure of neutrino Yukawa couplings assumed in eq. (19), the CP asymmetry ε in each case can be expressed as

$$\begin{aligned} &\text{(i)} \qquad \varepsilon \simeq -\frac{(-1+q_1)^2}{2(4p_1^2+1+q_1^2)} \frac{2\Delta_1 \tilde{\Gamma}_{N_1}}{4\Delta_1^2 + \tilde{\Gamma}_{N_1}^2} \sin 2(\varphi_3 - \varphi_1), \\ &\text{(ii)} \qquad \varepsilon \simeq -\frac{(1-q_2)^2}{2(p_2^2+1+q_2^2)} \frac{2\Delta_2 \tilde{\Gamma}_{N_2}}{4\Delta_2^2 + \tilde{\Gamma}_{N_2}^2} \sin 2(\varphi_3 - \varphi_2), \end{aligned} \tag{23}$$

where $\Delta_i = \frac{M_i}{M_3} - 1$ and $\tilde{\Gamma}_{N_i} = \frac{\Gamma_{N_i}}{M_i}$. These formulas show that the CP asymmetry ε could have large values for the case with $\Delta_i = O(\tilde{\Gamma}_{N_i})$ as long as both $q_{1,2} \neq 1$ and $\sin 2(\varphi_3 - \varphi_{1,2}) \neq 0$ are satisfied. As easily found, the CP phases appeared in eq. (23)

[12] The leptogenesis for the high mass right-handed neutrinos is possible also in this radiative mass model. In fact, such a possibility has been studied in [14] for the normal hierarchy and a similar result is expected for the inverted hierarchy. We are interested in the features of the TeV scale model here.

have no relation with the CP phase which controls the value of effective neutrino mass m_{ee} for the neutrinoless double β decay in eq. (28).

On the other hand, the washout of the generated lepton number asymmetry could be brought by both the lepton number violating 2-2 scattering such as $\eta\eta \to \ell_\alpha \ell_\beta$ and $\eta^\dagger \ell_\alpha \to \eta \bar{\ell}_\beta$ and also the inverse decay of N_i. However, if the relevant Yukawa couplings are small enough, these processes could be nearly freezed out before the temperature of the thermal plasma decreases to $T \lesssim M_3$. Thus, the washout of the generated lepton number asymmetry is expected to be suppressed sufficiently. In order to examine this quantitatively, we numerically solve the coupled Boltzmann equations for the number density of N_3 and the lepton number asymmetry. We introduce these number densities in the co-moving volume as $Y_{N_3} = \frac{n_{N_3}}{s}$ and $Y_L = \frac{n_\ell - n_{\bar{\ell}}}{s}$ by using the entropy density s. The Boltzmann equations for these are written as[13]

$$\begin{aligned}
\frac{dY_{N_3}}{dz} &= -\frac{z}{sH(M_3)} \left(\frac{Y_{N_3}}{Y_{N_3}^{\rm eq}} - 1 \right) \left\{ \gamma_D^{N_3} + \sum_{i=1,2} \left(\gamma_{N_3 N_i}^{(2)} + \gamma_{N_3 N_i}^{(3)} \right) \right\}, \\
\frac{dY_L}{dz} &= \frac{z}{sH(M_3)} \left\{ \varepsilon \left(\frac{Y_{N_3}}{Y_{N_3}^{\rm eq}} - 1 \right) \gamma_D^{N_3} - \frac{2Y_L}{Y_\ell^{\rm eq}} \left(\sum_{i=1,2} \frac{\gamma_D^{N_i}}{4} + \gamma_N^{(2)} + \gamma_N^{(13)} \right) \right\}, \qquad (24)
\end{aligned}$$

where $z = \frac{M_3}{T}$ and $H(M_3) = 1.66 g_*^{1/2} \frac{M_3^2}{m_{\rm pl}}$. The equilibrium values for these are expressed as $Y_{N_3}^{\rm eq}(z) = \frac{45}{2\pi^4 g_*} z^2 K_2(z)$ and $Y_\ell^{\rm eq} = \frac{45}{\pi^4 g_*}$, where $K_2(z)$ is the modified Bessel function of the second kind. In these equations we omit several processes whose contributions are considered to be negligible compared with others. We should note that the inverse decay to $N_{1,2}$ induced by the Yukawa couplings $h_{1,2}$ could cause a large contribution to the washout of the lepton number asymmetry since $M_i \simeq M_3$ is satisfied for $i = 1$ in case (i) and for $i = 2$ in case (ii).[14] In the Appendix, we present the relevant reaction density γ contained in these equations.

The baryon number asymmetry $Y_B (\equiv \frac{n_b - n_{\bar{b}}}{s})$ is transformed from the generated lepton number asymmetry through the sphaleron process. It is estimated by using the solution

[13]The $\Delta L = 2$ scattering reaction densities $\gamma_N^{(2)}$ and $\gamma_N^{(13)}$ involve the interference terms for the right-handed neutrinos with tiny mass splittings. Although they are suggested to play a crucial role in [28], its effect might be suppressed due to very small neutrino Yukawa couplings (16) of the lightest right-handed neutrino N_3.

[14]In the analysis of the resonant leptogenesis in [14], the inverse decay has not been taken into account. As the result, the required mass degeneracy for the right-handed neutrinos is underestimated by one order of magnitude there. In that case, however, it is still milder than the usual case.

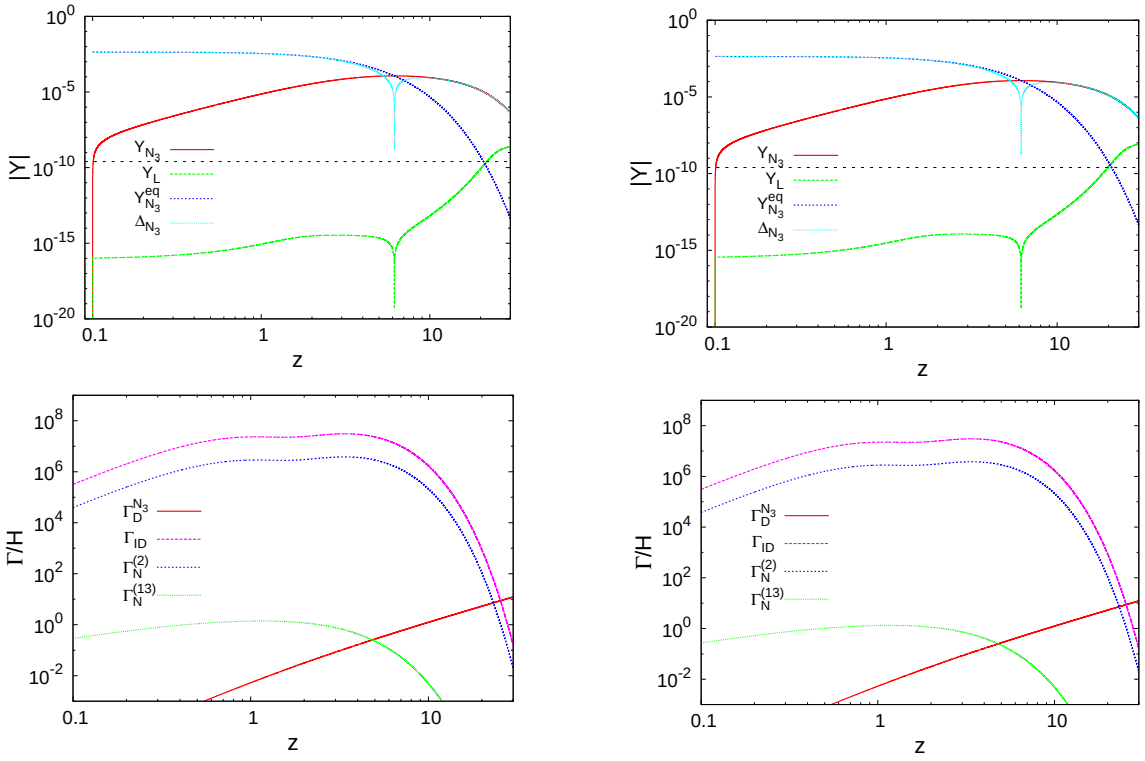

Fig. 3 The upper left and right panels show the evolution of the lepton number asymmetry $|Y_L|$ and the N_3 number density $|Y_{N_3}|$ for the cases (i) and (ii) given in Table 1 with $\Delta_i = 10^{-6.5}$. The lower panels show the ratio of the reaction rate of the lepton number violating processes to the Hubble parameter in each corresponding case.

of the coupled equations in eq. (24) as

$$Y_B = -\frac{8}{23} Y_L(z_{\rm EW}), \tag{25}$$

where we use $B = \frac{8}{23}(B-L)$ which is also satisfied in this model. The parameter $z_{\rm EW}$ is related to the sphaleron decoupling temperature $T_{\rm EW}$ through $z_{\rm EW} = \frac{M_3}{T_{\rm EW}}$ and $z_{\rm EW} \simeq 20$ in the present case. The solution of the Boltzmann equations is given in the upper panel of Fig. 3 for each case given in Table 1. The mass degeneracy Δ_i is fixed to $\Delta_i = 10^{-6.5}$. In this estimation, the CP phase $\varphi_3 - \varphi_{1,2}$ in eq. (23) is chosen to make ε a maximum value. From this figure, we find that the case (ii) gives a consistent solution with the required lepton number asymmetry for the assumed right-handed neutrino mass degeneracy. On the other hand, in the case (i) the generated baryon number asymmetry does not reach the required value by a small amount. Here we note that the value of ε is one order of magnitude larger in the case (ii) than that in the case (i). We note that this feature is

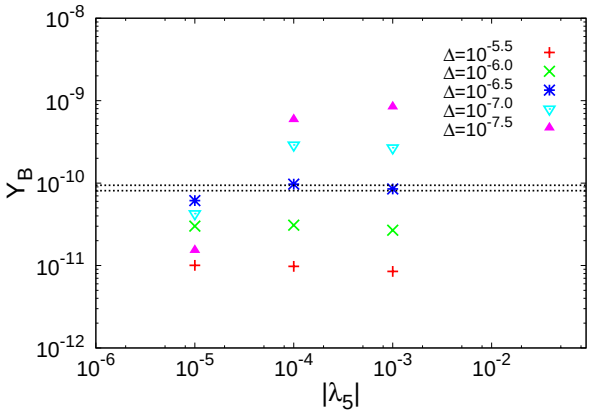

Fig. 4 The required mass degeneracy for the right-handed neutrinos to generate the sufficient baryon number asymmetry. We use the parameters in the case (ii) in this analysis.

caused by the neutrino mass matrix fixed by $p_{1,2}$ and $q_{1,2}$. If we use these solutions, we find that the model induces the baryon number asymmetry in each case as

$$\text{(i) } Y_B = 2.9 \times 10^{-11}, \qquad \text{(ii) } Y_B = 9.7 \times 10^{-11}. \tag{26}$$

If the CP phase takes a suitable value in the present parameter setting, the desirable value of Y_B can be obtained in the case (ii) even for milder degeneracy among the right-handed neutrinos compared with the ordinary resonant leptogenesis [27].

It is useful to see the behavior of the lepton number violating reaction rate in this analysis. The thermally averaged reaction rate is related to the reaction density through

$$\Gamma_D^{N_3} = \frac{\gamma_D^{N_3}}{n_{N_3}^{\rm eq}}, \qquad \Gamma_{\rm ID}^{N_{1,2}} = \frac{\gamma_D^{N_{1,2}}}{n_\ell^{\rm eq}}, \qquad \Gamma_N^{(2,13)} = \frac{\gamma_N^{(2,13)}}{n_\ell^{\rm eq}}, \tag{27}$$

for the decay of N_3 and the inverse decay of $N_{1,2}$ given in eq. (30), and for the 2-2 scattering processes given in eqs. (33) and (34), respectively. The ratio of the thermally averaged reaction rate to the Hubble parameter $\frac{\Gamma}{H}$ is plotted as a function of z in the lower panels of Fig. 3. These panels suggest that the lepton number violating processes show the almost same behavior in both cases. We find from these panels that the lepton number violating processes decouple at $z \gtrsim 20$ and then the washout of the generated lepton number asymmetry is suppressed sufficiently after this period in both case. The main reason to cause the difference in the generated lepton number asymmetry in both cases is considered to come from the difference in the value of the CP asymmetry ε, which shows the difference of one order of magnitude between these cases as addressed already.

We note that both the neutrino mass eigenvalues and the PMNS matrix does not change in this model as long as the value of $|h_{1,2}^2 \lambda_5|$ is kept to a suitable value. If we use this feature, we can vary the magnitude of the neutrino Yukawa couplings consistently with all the neutrino oscillation data by changing the value of $|\lambda_5|$. In Fig. 4, we show the required mass degeneracy Δ_2 between the right-handed neutrinos to generate the sufficient baryon number asymmetry for several $|\lambda_5|$ values in the case (ii). The figure shows that the sufficient baryon number asymmetry could be generated for $\Delta_2 \lesssim O(10^{-6.5})$ as long as $|\lambda_5|$ is in the region fixed by eq. (13). Although larger $|\lambda_5|$ makes $|h_2|$ smaller and then results in the smaller CP asymmetry, the washout due to the lepton number violating processes also become smaller. In much larger $|\lambda_5|$ region, the former suppression exceeds the latter effect. On the other hand, the smaller $|\lambda_5|$ makes $|h_2|$ larger to enhance both the CP asymmetry and the washout of the generated lepton number asymmetry. In much smaller $|\lambda_5|$ region, the latter enhancement exceeds the former effect. This explains the behavior of Y_B shown in this figure. The sufficient baryon number asymmetry could be generated only for a restricted region of $|\lambda_5|$. It is also clear from eq. (23) that the smaller Y_B is obtained for the smaller Δ_2 at the region of $|\lambda_5| < 10^{-5}$ where ε is expected to be proportional to $\Delta_2/\tilde{\Gamma}_{N_2}$. The similar behavior is obtained also in the case (i), although the severer mass degeneracy Δ_1 is required to generate the sufficient baryon number asymmetry.

The required mass degeneracy Δ_i is much milder compared with the resonant leptogenesis in the ordinary seesaw scenario at the TeV scale. It is useful to remind the reader that $\Delta = O(10^{-10\sim-8})$ is required to generate the sufficient baryon number asymmetry there. This interesting feature which is also found in the normal hierarchy case is brought by the neutrino mass generation mechanism in the model. Although the model is the simple extension of the SM, it can consistently explain three crucial problems in the SM, that is, the small masses and large mixing of neutrinos, the DM abundance and the baryon number asymmetry in the Universe, by fixing the parameters suitably.

3.2 DM detection and neutrinoless double β decay

Finally, we discuss the relation between the model and the low energy phenomena, in particular, the DM scattering with a nucleus and the neutrinoless double β decay. They are considered as the promising targets in the next generation experiments. One might

consider that eqs. (13) and (15) suggest that the inert doublet DM might be detected in the direct search experiments. If $|\lambda_5|$ is small enough within the bound (13), one might expect that it is detected through the inelastic scattering. However, since the DM velocity has the upper bound $v_{\rm esc}$ as discussed before, the inelastic scattering of the inert doublet DM is kinematically allowed only in the restricted parameter region. Xenon100 has already excluded this possibility as shown in Fig. 1.

In the elastic scattering case, on the other hand, if λ_3 and λ_4 take suitable values within (15), the inert doublet DM is expected to be found through the Xenon1T experiment. In Fig. 5, we plot the contours of the DM-nucleon scattering cross section σ_n^0 and also the contour of the expected sensitivity bound of Xenon1T [29] in the (m_η, λ_4) plane for both sign of λ_3. In the left panel, we plot them for $\lambda_3 = -0.4$ (red thin solid lines) and -0.01 (green thin dotted lines). The contour of $\sigma_n^0 = 4.4 \times 10^{-45}$ cm^2 is also plotted by using the same type of lines as these bounds for each λ_3. The upper shaded region could not be reached by Xenon1T and the lower shaded regions have been excluded by Xenon100. We find that the Xenon100 result excludes a substantial region in this plane for larger value of $|\lambda_3|$. In the right panel, λ_3 is fixed to 1.0 (red thin solid lines) and 0.4 (green thin dotted lines) and the contours of $\sigma_n^0 = 2 \times 10^{-45}$ and 4×10^{-46} cm^2 are plotted for each λ_3 in the same way as the left panel. The shaded region cannot be reached by Xenon1T. All region in the plane has not been excluded by Xenon100 in this case. In both panels, we also plot the contour of the required DM relic density $\Omega h^2 = 0.11$ by the thick lines of the same type as the ones used to plot the cross section for each value of λ_3. Thus, the cross section predicted by this model should be read off on these lines. This figure shows that our DM candidate is expected to be found in the Xenon1T experiment as long as $\lambda_{3,4}$ and m_η take suitable values. We should note that such parameters can be consistent with the ones which have been discussed in the previous part in relation to the neutrino oscillation data and leptogenesis.

The neutrinoless β decay could also be another future target of this model. The effective mass m_{ee} for the neutrinoless double β decay in this model is given by

$$\begin{aligned} m_{ee} &= \left| \sum_{i=1}^{3} U_{ei}^2 m_i \right| \simeq \left| (U_{e1}^2 + U_{e2}^2)\sqrt{\Delta m^2_{\rm atm}} - U_{e1}^2 \sqrt{\Delta m^2_{\rm sol}} \right| \\ &\simeq \sqrt{\Delta m^2_{\rm atm}} \left[U_{e1}^4 + U_{e2}^4 + 2U_{e1}^2 U_{e2}^2 \cos(\varphi_1 - \varphi_2) \right]^{1/2} . \end{aligned} \tag{28}$$

If we use the parameters obtained through the previous analysis, we can estimate the

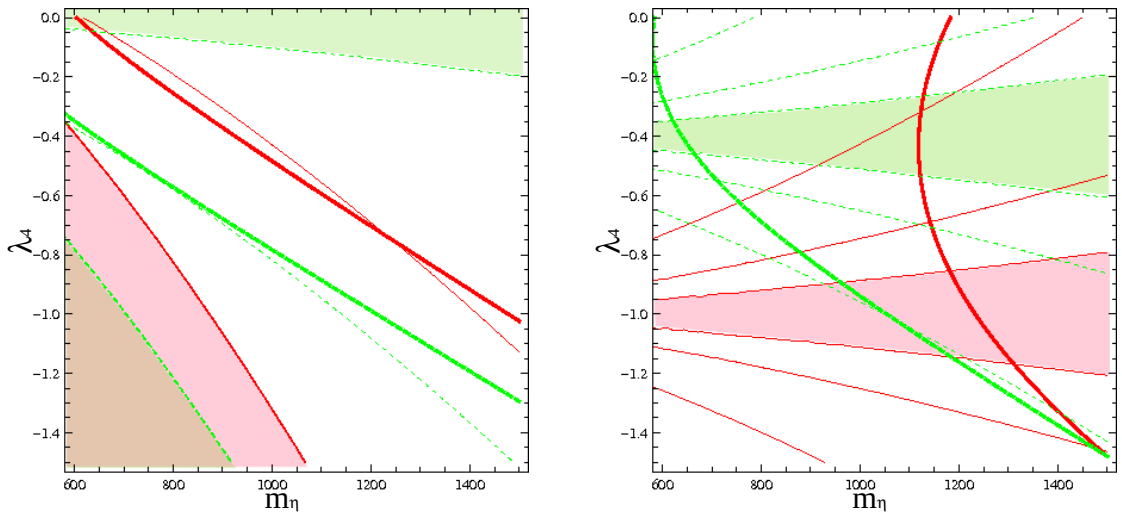

Fig. 5 Regions in the (m_η, λ_4) plane where the DM is expected through the direct search in Xenon1T experiment. The sign of λ_3 is fixed to $\lambda_3 < 0$ in the left panel and $\lambda_3 > 0$ in the right panel. The contours of σ_n^0, the sensitivity bound of Xenon1T, and also the contour of the DM relic density $\Omega h^2 = 0.11$ are also plotted. Detailed explanation of the lines can be found in the text. In this plot, we use $|\lambda_5| = 10^{-4}$.

value of m_{ee}, which is shown in the last column of Table 1. These values are obtained by changing the phases in the possible range. As usually expected in the inverted hierarchy case, we find that these values are contained in the region which could be observed in the next generation experiments.

Since the region of $|\lambda_5|$ is confined to rather restricted region through the DM search, we might have useful information on the order of degeneracy among the right-handed neutrinos by requiring the production of the observed baryon number asymmetry as discussed above. This might allow us more detailed study of the model by combining analysis of the neutrino oscillation data and the baryon number asymmetry. On the other hand, although the effective mass for the neutrinoless double β decay is related to λ_5 through the combination $|\lambda_5 h_{1,2}^2|$ which controls the neutrino mass eigenvalues, it is not directly related to $|\lambda_5|$ itself as found from eq. (28). The value of m_{ee} does not change even if we change the value of $|\lambda_5|$ as long as the flavor structure (19) is kept. This is quite different from the lepton flavor violating processes discussed in the previous part. As a result, even if we use the $|\lambda_5|$ value restricted by the DM direct search, the effective mass m_{ee} is not expected to be determined in more precise way.[15] The direct DM search seems to be a

[15]We should also note that the CP phases appeared in eqs.(28) and (23) have no direct relation.

promising experiment to examine the model other than the search of the charged scalars in the LHC.

4 Conclusion

We have constructed a concrete example to realize the inverted hierarchy of the neutrino masses in the radiative neutrino mass model at TeV scales. The model is an interesting and simple extension of the SM by adding an additional doublet scalar and three right-handed neutrinos only. In this example, we have examined the possibility for the simultaneous explanation of the neutrino oscillation data, the DM abundance and the baryon number asymmetry in the Universe. The results show that their simultaneous explanation is possible as long as the DM is identified with the lightest neutral component of the inert doublet scalar and the resonant leptogenesis is assumed.

In the resonant leptogenesis, the degeneracy required for the right-handed neutrinos is milder by a few order of magnitude than the one known in the ordinary resonant leptogenesis at TeV scales. This feature is brought about as a result of the present neutrino mass generation scheme. The right-handed neutrino spectrum also affects the resonant leptogenesis. This is caused by the flavor structure of the neutrino Yukawa couplings which is imposed by the neutrino oscillation data. The neutrinoless double β decay can be observed through the next generation experiments also in this inverted hierarchy model. The most promising experiment to examine the model may be the DM direct search. It is expected to be found in the Xenon1T experiment.

What DM is in this radiative neutrino mass model is closely related to a key parameter λ_5 of the model, which is also connected with both the neutrino mass generation and the production of the baryon number asymmetry. Thus, if a DM direct search could find some candidate, the model might be studied in more definite way based on it.

Acknowledgement

This work is partially supported by a Grant-in-Aid for Scientific Research (C) from Japan Society for Promotion of Science (No.24540263).

Appendix

We summarize the formulas of the reaction density used in the Boltzmann equations [30] for the number density of N_3 and the lepton number asymmetry.[16] In order to give the expression for the reaction density of the relevant processes, we introduce dimensionless variables

$$x = \frac{s}{M_3^2}, \qquad a_j = \frac{M_j^2}{M_3^2}, \qquad a_\eta = \frac{M_\eta^2}{M_3^2}, \tag{29}$$

where s is the squared center of mass energy. The reaction density for the decay of N_j can be expressed as

$$\gamma_D^{N_j} = \frac{(hh^\dagger)_{jj}}{8\pi^3} M_3^4 a_j \sqrt{a_j} \left(1 - \frac{a_\eta}{a_j}\right)^2 \frac{K_1(\sqrt{a_j} z)}{z}, \tag{30}$$

where $K_1(z)$ is the modified Bessel function of the second kind.

The reaction density for the scattering process is expressed as

$$\gamma(ab \to ij) = \frac{T}{64\pi^4} \int_{s_{\rm min}}^{\infty} ds\ \hat{\sigma}(s) \sqrt{s} K_1\left(\frac{\sqrt{s}}{T}\right), \tag{31}$$

where $s_{\rm min} = \max[(m_a + m_b)^2, (m_i + m_j)^2]$ and $\hat{\sigma}(s)$ is the reduced cross section. In order to give the concrete expression for the reaction density relevant to eq. (24), we define the following quantities for convenience:

$$\begin{aligned}
&\frac{1}{D_i(x)} = \frac{x - a_i}{(x - a_i)^2 + a_i^2 c_i}, \qquad c_i = \frac{1}{64\pi^2} \left(\sum_{\alpha = e,\mu,\tau} |h_{\alpha i}|^2\right)^2 \left(1 - \frac{a_\eta}{a_i}\right)^4, \\
&\lambda_{ij} = \left[x - (\sqrt{a_i} + \sqrt{a_j})^2\right] \left[x - (\sqrt{a_i} - \sqrt{a_j})^2\right], \\
&L_{ij} = \ln\left[\frac{x - a_i - a_j + 2a_\eta + \sqrt{\lambda_{ij}}}{x - a_i - a_j + 2a_\eta - \sqrt{\lambda_{ij}}}\right], \\
&L'_{ij} = \ln\left[\frac{\sqrt{x}(x - a_i - a_j - 2a_\eta) + \sqrt{\lambda_{ij}(x - 4a_\eta)}}{\sqrt{x}(x - a_i - a_j - 2a_\eta) - \sqrt{\lambda_{ij}(x - 4a_\eta)}}\right].
\end{aligned} \tag{32}$$

As the lepton number violating scattering processes induced through the N_i exchange,

[16] These formulas are the same as the ones given in the Appendix of [14] except that they are arranged so as to be applicable to the mass spectrum assumed in this paper. Typos and errors are corrected.

we have

$$\hat{\sigma}_N^{(2)}(x) = \frac{1}{2\pi}\frac{(x-a_\eta)^2}{x^2}\left[\sum_{i=1}^{3}(hh^\dagger)_{ii}^2\frac{a_i}{x}\left\{\frac{x^2}{xa_i-a_\eta^2}+\frac{x}{D_i(x)}+\frac{(x-a_\eta)^2}{2D_i(x)^2}\right.\right.$$
$$- \frac{x^2}{(x-a_\eta)^2}\left(1+\frac{x+a_i-2a_\eta}{D_i(x)}\right)\ln\left(\frac{x(x+a_i-2a_\eta)}{xa_i-a_\eta^2}\right)\Bigg\}$$
$$+ \sum_{i>j}\mathrm{Re}[(hh^\dagger)_{ij}^2]\frac{\sqrt{a_ia_j}}{x}\left\{\frac{x}{D_i(x)}+\frac{x}{D_j(x)}+\frac{(x-a_\eta)^2}{D_i(x)D_j(x)}\right.$$
$$+ \frac{x^2}{(x-a_\eta)^2}\left(\frac{2(x+a_i-2a_\eta)}{a_j-a_i}-\frac{x+a_i-2a_\eta}{D_j(x)}\right)\ln\frac{x(x+a_i-2a_\eta)}{xa_i-a_\eta^2}$$
$$+ \left.\left.\frac{x^2}{(x-a_\eta)^2}\left(\frac{2(x+a_j-2a_\eta)}{a_i-a_j}-\frac{x+a_j-2a_\eta}{D_i(x)}\right)\ln\frac{x(x+a_j-2a_\eta)}{xa_j-a_\eta^2}\right\}\right] \quad (33)$$

for $\ell_\alpha\eta^\dagger \to \bar{\ell}_\beta\eta$ and also

$$\hat{\sigma}_N^{(13)}(x) = \frac{1}{2\pi}\left[\sum_{i=1}^{3}(hh^\dagger)_{ii}^2\left\{\frac{a_i(x^2-4xa_\eta)^{1/2}}{a_ix+(a_i-a_\eta)^2}\right.\right.$$
$$+ \left.\frac{a_i}{x+2a_i-2a_\eta}\ln\left(\frac{x+(x^2-4xa_\eta)^{1/2}+2a_i-2a_\eta}{x-(x^2-4xa_\eta)^{1/2}+2a_i-2a_\eta}\right)\right\}$$
$$+ \sum_{i>j}\mathrm{Re}[(hh^\dagger)_{ij}^2]\frac{\sqrt{a_ia_j}}{x+a_i+a_j-2a_\eta}$$
$$\times \left\{\frac{2x+3a_i+a_j-4a_\eta}{a_j-a_i}\ln\left(\frac{x+(x^2-4xa_\eta)^{1/2}+2a_i-2a_\eta}{x-(x^2-4xa_\eta)^{1/2}+2a_i-2a_\eta}\right)\right.$$
$$+ \left.\left.\frac{2x+a_i+3a_j-4a_\eta}{a_i-a_j}\ln\left(\frac{x+(x^2-4xa_\eta)^{1/2}+2a_j-2a_\eta}{x-(x^2-4xa_\eta)^{1/2}+2a_j-2a_\eta}\right)\right\}\right] \quad (34)$$

for $\ell_\alpha\ell_\beta \to \eta\eta$. The cross terms has no contribution if the CP phases are assumed to satisfy $|\sin 2(\varphi_{1,2}-\varphi_3)| = 1$. We adopt this possibility in the numerical analysis, for simplicity. Since another type of the lepton number violating process $N_iN_j \to \ell_\alpha\ell_\beta$ induced by the η exchange could be suppressed for a small $|\lambda_5|$, we can neglect them safely for the value of $|\lambda_5|$ used in this analysis.

As the lepton number conserving scattering processes which contribute to determine the number density of N_3, we have

$$\hat{\sigma}_{N_iN_j}^{(2)}(x) = \frac{1}{4\pi}\left[(hh^\dagger)_{ii}(hh^\dagger)_{jj}\left\{\frac{\sqrt{\lambda_{ij}}}{x}\left(1+\frac{(a_i-a_\eta)(a_j-a_\eta)}{(a_i-a_\eta)(a_j-a_\eta)+xa_\eta}\right)\right.\right.$$
$$+ \left.\left.\frac{a_i+a_j-2a_\eta}{x}L_{ij}\right\} - \mathrm{Re}[(hh^\dagger)_{ij}^2]\frac{2\sqrt{a_ia_j}L_{ij}}{x-a_i-a_j+2a_\eta}\right] \quad (35)$$

for $N_i N_j \to \ell_\alpha \bar{\ell}_\beta$ which are induced through the η exchange and also

$$\begin{aligned}\hat{\sigma}^{(3)}_{N_i N_j}(x) &= \frac{1}{4\pi}\frac{(x-4a_\eta)^{1/2}}{x^{1/2}}\left[|(hh^\dagger)_{ij}|^2\left\{\frac{\sqrt{\lambda_{ij}}}{x}\Big(-2\right.\right. \\ &+ \left.\left.\frac{a_\eta(a_i-a_j)^2}{(a_\eta-a_i)(a_\eta-a_j)x+(a_i-a_j)^2 a_\eta}\Big)+\frac{x^{1/2}}{(x-4a_\eta)^{1/2}}\left(1-2\frac{a_\eta}{x}\right)L'_{ij}\right\}\right. \\ &- \left.2\mathrm{Re}[(hh^\dagger)^2_{ij}]\frac{\sqrt{a_i a_j}(a_i+a_j-2a_\eta)L'_{ij}}{x(x-a_i-a_j-2a_\eta)}\right] \qquad (36)\end{aligned}$$

for $N_i N_j \to \eta\eta^\dagger$ which are induced through the ℓ_α exchange. The cross terms in these reduced cross sections can be neglected if the same assumption is made for the CP phases as eqs. (33) and (34).

References

[1] Super-Kamiokande Collaboration, Y. Fukuda, *et al.*, Phys. Rev. Lett. **81** (1998) 1562; SNO Collaboration, Q. R .Ahmad, *et al.*, Phys. Rev. Lett. **89** (2002) 011301; KamLAND Collaboration, K. Eguchi, *et al.*, Phys. Rev. Lett. **90** (2003) 021802; K2K Collaboration, M. H. Ahn, *et al.*, Phys. Rev. Lett. **90** (2003) 041801.

[2] WMAP Collaboration, D. N. Spergel, *et al.*, Astrophys. J. **148** (2003) 175; SDSS Collaboration, M. Tegmark, *et al.*, Phys. Rev. **D69** (2004) 103501.

[3] E. Ma, Phys. Rev. **D73** (2006) 077301.

[4] J. Kubo, E. Ma and D. Suematsu, Phys. Lett. **B642** (2006) 18.

[5] J. Kubo and D. Suematsu, Phys. Lett. **B643** (2006) 336; D. Suematsu, T. Toma and T. Yoshida, Phys. Rev. **D79** (2009) 093004; D. Suematsu, T. Toma and T. Yoshida, Phys. Rev. **D82** (2010) 013012.

[6] D. Aristizabal Sierra, J. Kubo, D. Restrepo, D. Suematsu and O. Zapata, Phys. Rev. **D79** (2009) 013011.

[7] E. Ma, Annals Fond. Broglie **31** (2006) 285; H. Fukuoka, J. Kubo and D. Suematsu, Phys. Lett. **B678** (2009) 401; D. Suematsu and T. Toma, Nucl. Phys. **B847** (2011) 567; H. Fukuoka, D. Suematsu and T. Toma, JCAP **07** (2011) 001.

[8] M. Fukugita and T. Yanagida, Phys. Lett. **B174** (1986) 45.

[9] M. Plümacher, Nucl. Phys. **B530** (1998) 207; W. Buchmüller and M. Plümacher, Int. J. Mod. Phys. **A15** (2000) 5047; W. Buchmüller, P. Di Bari, and M. Plümacher, Phys. Lett. **B547** (2002) 128; Nucl. Phys. **B643** (2002) 367; Nucl. Phys. **B665** (2003) 445; G. F. Giudice, A. Notari, M. Raidal, A. Riotto and A. Struma, Nucl. Phys. **B685** (2004) 89; W. Buchmüller, R. D. Peccei and T. Yanagida, Ann. Rev. Nucl. Part. Sci. **55** (2005) 311.

[10] D. Suematsu, Eur. Phys. J.**C56** (2008) 379; H. Higashi, T. Ishima and D. Suematsu, Int. J. Mod. Phys. **A26** (2001) 995; D. Suematsu, Phys. Rev. **D85** (2012) 073008.

[11] D. Suematsu, Eur. Phys. J.**C72** (2008) 1951.

[12] R. Barbieri, L. J. Hall and V. S. Rychkov, Phys. Rev. **D74** (2006) 015007; M. Cirelli, N. Fornengo and A. Strumia, Nucl. Phys. **B753** (2006) 178; L. L. Honorez, E. Nezri, J. F. Oliver and M. H. G. Tytgat, JCAP **0702** (2007) 028; Q.-H. Cao and E. Ma, Phys. Rev. **D76** (2007) 095011; S. Andreas, M. H. G. Tytgat and Q. Swillens, JCAP **0904** (2009) 004; E. Nezri, M. H. G. Tytday and G. Vertongen, JCAP **0904** (2009) 014; L. L. Honorez, JCAP **1101** (2011) 002.

[13] T. Hambye, F.-S. Ling, L. L. Honorez and J. Roche, JHEP **07** (2009) 090.

[14] S. Kashiwase and D. Suematsu, Phys. Rev. **D86** (2012) 053001.

[15] T2K Collaboration, K. Abe, *et al.*, Phys. Rev. Lett. **107** (2011) 041801; Double Chooz Collaboration, Y. Abe, *et al.*, Phys. Rev. Lett. **108** (2012) 131801; RENO Collaboration, J. K. Ahn, *et al.*, Phys. Rev. Lett. **108** (2012) 191802; The Daya Bay Collaboration, F. E. An, *et al.*, Phys. Rev. Lett. **108** (2012) 171803.

[16] K. Nakamura *et al.* (Particle Data Group), J. Phys. G 37 (2010) 075021.

[17] D. V. Forero, M. Tórtola and J. Valle, arXiv:1205.4018.

[18] CDMS Collaboration, Z. Ahmed, *et al.*, Phys. Rev. Lett. **102** (2009) 011301; XENON100 Collaboration, E. Aprile, *et al.*, Phys. Rev. Lett. **105** (2010) 131302.

[19] G. Angloher *et al.*, Astropart. Phys. **31** (2009) 270; V. N. Lebedenko *et al.*, Phys. Rev. **D80** (2009) 052010.

[20] G. Jungman, M. Kamionkowski and K. Griest, Phys. Rep. **267** (1996) 195.

[21] D. Smith and N. Weiner, Phys. Rev. **D64** (2001) 043502.

[22] Y. Cui, D. E. Marrissey, D. Poland and L. Randall, JHEP **0905** (2009) 076; C. Arina, F.-S. Ling and M. H. G. Tytgat, JCAP **0910** (2009) 018.

[23] M. B. Gavela, T. Hambye, D. Hernandez and P. Hernandez, JHEP **0909** (2009) 038; D. A. Sierra, A. Degee and J. F. Kamenik, JHEP **1207** (2012) 135.

[24] E. Ma and M. Raidal, Phys. Rev. Lett. **87** (2001) 011802.

[25] MEG collaboration, J. Adam *et al.*, Nucl. Phys. **B834** (2010) 1; BABAR collaboration, B. Aubert *et al.*, Phys. Rev. Lett. **104** (2010) 021802.

[26] K.Hagiwara, A. D. Martin, D. Nomura and T.Teubner, Phys. Lett. **B649** (2007) 173.

[27] M. Flanz, E. A. Pascos and U. Sarkar, Phys. Lett. **B345** (1995) 248; L. Covi, E. Roulet and F. Vissani, Phys. Lett. **B384** (1996) 169; A. Pilaftsis, Phys. ReV. **D56** (1997) 5431; E. Akhmedov, M. Frigerio and A. Yu Smirnov, JHEP **0309** (2003) 021; C. H. Albright and S. M. Barr, Phys. Rev. **D69** (2004) 073010; T. Hambye,J. March-Russell and S. W. West, JHEP **0407** (2004) 070; A. Pilaftsis and E. J. Underwood, Nucl. Phys. **B692** (2004) 303; A. Pilaftsis and E. J. Underwood, Phys. Rev. **D72** (2005) 113001.

[28] S. Blanchet, T. Hambye and F.-X.J.-Michaux, arXiv:0912.3153 [hep-ph].

[29] For example, E. Aprile, arXiv:1206.6288 [astro-ph.IM]

[30] M. Luty, Phys. Rev. **D45** (1992) 455; M. Plumacher, Nucl. Phys. **B530** (1998) 207.